

Electronic structure and exchange interactions in cobalt-phthalocyanine chainsWei Wu,^{1,*} N. M. Harrison,² and A. J. Fisher³¹*Department of Materials and London Centre for Nanotechnology, Imperial College London, South Kensington Campus, London, SW7 2AZ, United Kingdom*²*Department of Chemistry and London Centre for Nanotechnology, Imperial College London, South Kensington Campus, London, SW7 2AZ, United Kingdom*³*UCL Department of Physics and Astronomy and London Centre for Nanotechnology, University College London, Gower Street, London, WC1E 6BT, United Kingdom*

(Received 8 October 2012; revised manuscript received 2 May 2013; published 26 July 2013)

The magnetic properties and electronic structure of cobalt phthalocyanine (CoPc, $\text{spin-}\frac{1}{2}$) molecular chains have been studied using density functional theory with a hybrid exchange functional, over a wide range of chain geometries. Our theoretical results for the exchange interactions in the known phases α -CoPc ($J/k_B \sim 85$ K) and β -CoPc ($J/k_B \sim 2$ K) are in quantitative agreement with recent magnetic measurements; we also find the computed exchange interaction agrees qualitatively with recent measurements by inelastic tunneling spectroscopy on thin films. The computed exchange interactions are much larger than those in copper phthalocyanine (CuPc), and are predicted to rise to a maximum of $J/k_B \sim 400$ K when the molecules are face-on. The dominant exchange mechanism is expected to be superexchange arising from the direct hopping between d_{z^2} orbitals.

DOI: [10.1103/PhysRevB.88.024426](https://doi.org/10.1103/PhysRevB.88.024426)

PACS number(s): 75.50.Xx, 71.15.Mb, 71.20.Rv, 75.30.Et

I. INTRODUCTION

Spin-bearing transition-metal phthalocyanines (TMPc), in which a divalent transition-metal ion is located at the center of a conjugated phthalocyanine ring, have attracted much attention^{1–5} recently. This family of organic materials has several interesting features: They are organic semiconductors that can be prepared in bulk crystalline and thin-film forms as well as in nanowires,² they can be used to fabricate organic field-effect transistors (OFETs),⁶ they show magnetic order that can be tuned by changing the molecular arrangement,⁵ and (at least in some cases) they can have very long spin-lattice relaxation times as observed in other organic materials,⁷ despite the presence of the transition metal. For example, in copper-phthalocyanines (CuPc), the spin-lattice relaxation time is up to $1 \mu\text{s}$ ⁸ at low temperature. These properties make TMPcs promising candidates both for quantum information processing and for more conventional spintronic applications.⁹

The best studied example, both theoretically and experimentally, is CuPc.^{2,5} In that case the dominant magnetic and electronic interactions are along chains of molecules which are stacked facing one another, but the computed nearest-neighbor exchange interaction rises only up to 4 K (antiferromagnetic) even when the molecules are oriented directly face-on (stacking angle equal to 90° ⁵). The experimentally accessible examples have structures with molecules tilted from the ideal face-on geometry, lower exchange interactions, and correspondingly lower transition temperatures.^{1,2} It would be very desirable to have organic magnets in this class with higher ordering temperatures for a range of applications including quantum information processing^{7,9} and molecular spintronics,^{10,11} and hence to understand how far the exchange interaction can be increased by engineering the transition metal or ligand. This in turn requires knowledge of the underlying interaction mechanism for the exchange coupling.¹²

CoPc ($\text{C}_{32}\text{H}_{16}\text{N}_8\text{Co}$) shown in Fig. 1 is an especially interesting example in this respect, because inelastic electron

tunneling in a scanning tunneling microscope (STM)³ suggests a very large energy scale for local spin excitations up to approximately 18 ± 2 meV ($\sim 209 \pm 20$ K). It is tempting to identify this as a nearest-neighbor exchange interaction, and if this is correct CoPc should have a much higher magnetic ordering temperature than other TMPcs.¹³ CoPc molecules deposited on the Au(111) surface have been studied using STM; it was shown that in its intact form the molecule's magnetic moment is quenched by the interaction with the metal, the moment can be restored by removing eight hydrogen atoms from the molecule at which point the current-voltage spectra displays a Kondo effect.¹⁴ The properties of the Kondo signal can be understood on the basis of a simple model in which the unpaired molecular spin resides in the out-of-plane $3d_{z^2}$ orbital on the central Co atom, which hybridizes with the $6s$ states of the underlying Au atoms.¹⁵ This suggests that the unpaired electron spin on the CoPc molecule can couple strongly to neighbors perpendicular to the molecular plane. Although there have been a number of calculations of the electronic structure of isolated CoPc molecules or single molecules adsorbed on surfaces,^{14,16–20} the important issues of the magnitude, sign, variation with the stacking geometry, and exchange coupling mechanism have not so far been addressed.

In this paper we present a systematic theoretical study of the magnetic properties and electronic structure of CoPc in a one-dimensional chain geometry using hybrid exchange density functional theory which is abbreviated to HDFT in what follows. This geometry enables us to focus on the dominant intrachain electronic and magnetic interactions. In Sec. II we give a brief introduction to the computational tools used. In Sec. III we analyze the molecular geometries in the chains and introduce the concepts of stacking and sliding angles to parametrize the nearest-neighbor interaction. In Sec. IV we report our calculated exchange interactions as a function of geometry and show how they are related to the electronic structure. Finally, in Sec. V we will draw some more general conclusions.

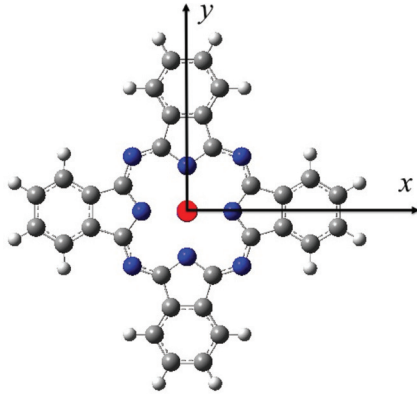


FIG. 1. (Color online) The molecular structure of cobalt phthalocyanine (CoPc). Co is in red, N is in pure blue, C is in gray, and H is in white. The molecule has D_{4h} symmetry.

II. COMPUTATIONAL METHODS

We have carried out unrestricted calculations for isolated CoPc molecules using HDFT with a 6-31G basis set²¹ in the GAUSSIAN09 code.²² A 6-31 + G* basis set²¹ is also used to test the sensibility of the basis set. Time-dependent density function theory (TD-DFT)^{23,24} with the 6-31G basis set is used here to calculate the excitation energy. The electronic structures of CoPc periodic chains were also calculated using HDFT in the unrestricted formalism as implemented in the CRYSTAL09 code,²⁵ with two molecules per unit cell in order to allow for the development of a magnetic superlattice. The Monkhorst-Pack sampling²⁶ of reciprocal space is carried out by choosing a grid of shrinking factor equal to eight. The truncation of the Coulomb and exchange series in direct space is controlled by setting the Gaussian overlap tolerance criteria to 10^{-6} , 10^{-6} , 10^{-6} , 10^{-6} , and 10^{-12} .²⁵ The self-consistent field (SCF) procedure is converged to a tolerance of 10^{-6} a.u. per unit cell (p.u.c). To accelerate convergence of the SCF process, all the calculations have been performed adopting a linear mixing of Fock matrices by 30%.

Electronic exchange and correlation are described using the B3LYP hybrid exchange-correlation functional²⁷ for both the calculations of single molecules and molecular chains. The advantages of B3LYP include a partial elimination of the self-interaction error and a balancing of the tendencies to delocalize and localize one-electron wave functions by mixing Fock exchange with that from a generalized gradient approximation (GGA) exchange functional.²⁷ B3LYP, as implemented in CRYSTAL, has previously been shown to provide an accurate description of the electronic structure and magnetic properties for both inorganic and organic compounds.^{4,5,28-32}

The van der Waals forces are important for determining the geometry of a CoPc molecular crystal. Therefore, a long-range dispersion correction for DFT developed by Grimme³³ and implemented in CRYSTAL09²⁵ is combined with the B3LYP exchange-correlation functional in order to optimize the interplanar lattice constant.

The broken-symmetry method³⁴ is used to localize anti-aligned spins on each molecule in order to describe the antiferromagnetic state. The magnetic excitations were then

described by a one-dimensional Heisenberg spin- $\frac{1}{2}$ chain³⁵

$$\hat{H} = 2J \sum_i \hat{S}_i \cdot \hat{S}_{i+1}, \quad (1)$$

with the exchange constant J estimated from the electronic structure calculations as

$$J = (E_{\text{FM}} - E_{\text{AFM}})/2, \quad (2)$$

where E_{AFM} and E_{FM} are the total energies of the two-molecule supercell in which the spin configurations are antiferromagnetic (AFM, i.e., spins anti-aligned) and ferromagnetic (FM, spins aligned), respectively. Note that with our sign convention a positive J corresponds to an interaction favoring the antiferromagnetic state (i.e., $E_{\text{AFM}} < E_{\text{FM}}$).

III. MOLECULAR GEOMETRY

The intramolecular coordinates were determined by the optimization of an isolated CoPc molecule. CoPc crystals are known to consist of parallel molecular planes along the stacking axis connecting Co atoms. As shown in Fig. 2 we first define d as the interplane distance and \hat{r} as the projection into the molecular plane of the vector joining the central Co atoms of the two molecules. Then we define the stacking angle ϕ as the angle between the molecular plane and the stacking axis connecting the Co atoms, and the sliding angle ψ as the angle between \hat{r} and the X axis as shown in Fig. 2. These two angles are related to the Cartesian coordinates X and Y defining the in-plane displacement of one Co atom relative to the next (Fig. 2) as $X = d \cot \phi \cos \psi$ and $Y = d \cot \phi \sin \psi$.

Since widely used exchange-correlation functionals, including B3LYP, do not describe van der Waals forces reliably, we have included an empirical dispersion energy correction³³ to the B3LYP functional in order to optimize the lattice

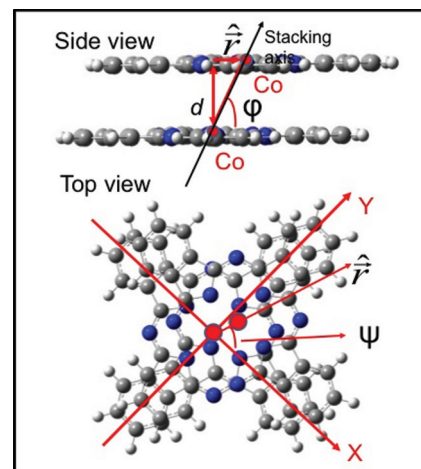


FIG. 2. (Color online) Two neighboring CoPc molecules from a side view and a top view to illustrate important geometrical parameters in the crystal structure. The atoms are color coded, i.e., Co is in red, C is in gray, N is in blue, and H is in white. The interplane distance is labeled as d , the stacking angle ϕ , and the sliding angle ψ . The stacking axis is indicated by a black arrow connecting Co atoms. The vector \hat{r} and the X and Y axes are used to define the sliding angle, i.e., $\cos \psi = \hat{r} \cdot \hat{X}$.

constant and hence the interplane distance. In the following calculations for exchange interactions, we first fix the interplane distance d at the experimentally determined value of 3.42 \AA ,^{36,37} then use the corrected functional to optimize the lattice constant for the experimentally relevant cross phases (for which the sliding angle is equal to 45°). In this way we can understand both how the van der Waals forces change the geometry and how this affects the exchange interactions. So far two phases of CoPc molecular crystals have received extensive experimental study: the α phase with stacking angle $\phi \simeq 66^\circ$ and sliding angle $\psi \simeq 45^\circ$, and the β phase with stacking angle $\phi \simeq 45^\circ$ and sliding angle $\psi \simeq 45^\circ$.^{36,37} In the thin films studied by STM,³ the stacking angle is inferred to be $60 \pm 3^\circ$ and after the first two layers the molecules are observed to stack directly atop one another (sliding angle 0°). CuPc has also been observed to form nanowires² in the η phase having a stacking angle of $\sim 63^\circ$ and a sliding angle of $\sim 27^\circ$ —the chemical similarity between the molecules makes it likely that this phase also exists in CoPc, although it has not yet been reported. Our HDFT approach gives us the freedom to vary the stacking, sliding angles, and the optimized Co-Co distance arbitrarily to give a wider range of chain structures beyond those currently known to be realized in nature. Accordingly, calculations have been performed for a range of stacking angles from 20° to 90° and sliding angles from 0° to 45° with 5° increments, exploiting the D_{4h} symmetry of the CoPc molecule. The rotation of molecular planes relative to one another about the stacking axis, as seen in, e.g., the x phase of lithium phthalocyanine (LiPc)³⁸ is not considered in the present paper as so far as there is no experimental observation for this type of geometry in CoPc.

IV. RESULTS AND DISCUSSION

A. Single CoPc molecules

In a D_{4h} environment, the five d orbitals, d_{z^2} , d_{xz} , d_{yz} , d_{xy} , and $d_{x^2-y^2}$ are split into a_{1g} , e_{gx} , e_{gy} , b_{2g} , and b_{1g} symmetries, respectively. When the orbital splittings are large compared to the on-site Coulomb energies, the d^7 configuration of Co^{2+} is expected to form a low-spin state with a single unpaired electron ($S = \frac{1}{2}$). The b_{1g} orbital is lifted very high in energy by the crystal field, so the unpaired electron can occupy one of the a_{1g} , e_g , or b_{2g} orbitals. We find the ground state of the molecule to be the A_{1g} state where the a_{1g} (d_{z^2}) orbital is singly occupied. The energy level alignments for Kohn-Sham orbitals along with their eigenvalues near the HOMO (highest occupied molecular orbital)-LUMO (lowest unoccupied molecular orbital) gap in this state are shown schematically in Fig. 3; except for the high-lying b_{1g} orbital (not shown), the d -orbital energies lie somewhat below the highest occupied a_{1u} orbital of the Pc ring. The singly occupied molecular orbital (SOMO) arises from a rather weak hybridization between the dominant a_{1g} (d_{z^2}) atomic orbital and the ligand $1s$, $2s$, p_x , and p_y orbitals. The spatial distribution of the orbital is shown in Fig. 4.

1. The ground state

The Mulliken charge on the Co atom is approximately $+1.1|e|$, similar to that found for the Cu atom in CuPc with a

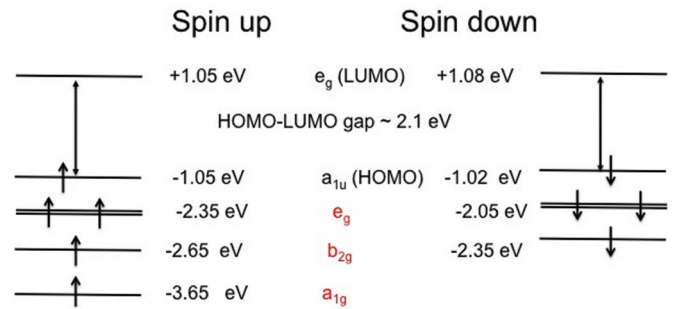


FIG. 3. (Color online) The Kohn-Sham eigenvalues in the A_{1g} ground state along with their irreducible representations of D_{4h} symmetry near the HOMO-LUMO gap are shown. The spin-up eigenvalues are on the left and the spin-down on the right. Orbitals derived from d states are shown in red. The HOMO-LUMO gap is approximately 2.1 eV. The zero of energy is chosen to be in the middle of the HOMO-LUMO gap for spin-up.

similar basis set⁴ but larger than the $+0.59|e|$ previously reported for CoPc¹⁷ (though the use of a different basis set means the results are not strictly comparable). This is consistent with a Co formal charge state of $+2|e|$ accompanied by hybridization between the π system of the Pc and the Co d orbitals. The computed HOMO-LUMO gap is approximately 2 eV, which is similar to that computed for the copper phthalocyanine molecule; this is not surprising, as the HOMO and LUMO are dominated by ligand orbitals in both cases.⁴ The computed HOMO-LUMO gap for CoPc is also comparable with the measured optical gap, i.e., the Q -band wavelength $\sim 600 \text{ nm}$ ($\sim 2.1 \text{ eV}$) seen in optical absorption spectra.⁴⁰ Our TD-DFT calculations show that the first two dipole-allowed excitations with symmetry E_u arise from the HOMO-LUMO transition and have excitation energy $\sim 2.1 \text{ eV}$. This is in agreement with the HOMO-LUMO gap computed in the single molecule calculation. By comparing the energies of the occupied spin-up and unoccupied spin-down a_{1g} orbitals, we can estimate the

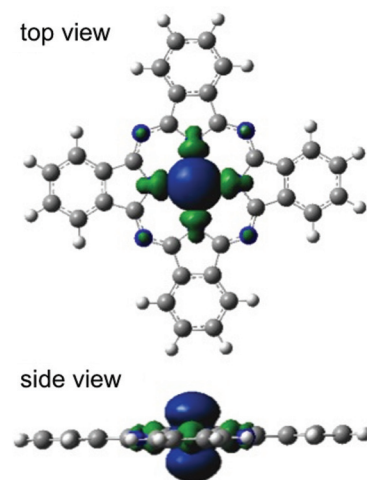


FIG. 4. (Color online) The top view (a) and side view (b) of the singly occupied orbital a_{1g} isosurfaces (isoval = 0.01 a.u.) in the ground state of a CoPc isolated molecule are shown. The sign of a_{1g} orbital is color coded, i.e., positive in red and negative in green. The color scheme for atoms is the same as that in Fig. 1.

on-site Coulomb interaction U for the a_{1g} orbital. We find a value of $U \sim 6.0$ eV, which is substantially larger than the corresponding quantity for CuPc ($U \sim 4.0$ eV).⁵ This is to be expected because in our calculations the SOMO for CoPc is more localized than the singly occupied b_{1g} state in CuPc. This large effective U also explains why the configuration shown in Fig. 3 is stable despite the Kohn-Sham eigenvalue of the a_{1g} state lying more than 1.5 eV below the a_{1u} state of the Pc ring. The authors in Ref. 19 have used DFT + U methods to compute the electronic structure of an isolated CoPc molecule. They found that the result with $U = 6$ eV best fitted the experimentally observed structural parameters, valence band spectrum of the CoPc molecule, and their HDFT calculations using the B3LYP functional. Our estimate for U is therefore in agreement with that reported in Ref. 19.

Previous work has led to various conclusions about the nature of the ground state in isolated CoPc. Early $X\alpha$ calculations with a restricted numerical basis set derived from atomic and ionic calculations also found a ground state with A_{1g} symmetry.¹⁶ In Ref. 18 a combination of polarization-dependent x-ray absorption spectroscopy (XAS) for CoPc adsorbed on Au and semiempirical ligand-field calculations were used to determine the electronic structure of the CoPc molecule. The ligand-field approach may give a good representation of the local d -orbital physics, but describes the ligands only approximately. They found that the XAS spectra could be interpreted in terms of an A_{1g} ground state dominated by the a_{1g} orbital. The ground state calculated here is therefore consistent with the XAS spectra reported in Ref. 18. The calculations in Ref. 19 were performed with both the HDFT and GGA + U approaches; the value of U was taken to be 6 eV, in agreement with our estimate, and it was found that the e_g single-particle states are both fully occupied (consistent with a A_{1g} ground state). Finally, as discussed above, the A_{1g} ground state agrees with the interpretation¹⁵ of the interactions leading to the formation of the Kondo singlet in CoPc on Au(111).¹⁴ CoPc monolayer calculations based on GGA functionals uncorrected for on-site electron correlation²⁰ also find the A_{1g} ground state. The anisotropy of the g factor in electron paramagnetic resonance has been interpreted in terms of an A_{1g} ground state.³⁹ On the other hand, DFT calculations using uncorrected GGA functionals and a local triple- ζ quality Slater-type basis set¹⁷ found that an 2E_g configuration is the lowest in energy, with the ${}^2A_{1g}$ configuration approximately 0.1 eV higher in energy. The two main differences with the calculations reported here are the local basis set and the DFT functional adopted; in order to estimate the sensitivity of our calculations to the basis set we have repeated our calculations with a 6-31 + G* basis (containing an additional diffuse polarization function for each atom); the ground state is unchanged. It seems highly likely that the ground state of CoPc is well approximated by an A_{1g} ground state and that the correct description of this state in electronic structure calculations requires an estimate of the on-site electron correlation as provided by the HDFT or DFT + U approaches.

2. The first orbital excited state

The energies of states with e_g or b_{2g} orbitals singly occupied can be estimated by attempting to converge an unconstrained SCF calculation starting from a density matrix

with these occupation patterns. The single occupation of an e_g state induces an orbital degeneracy and hence a Jahn-Teller distortion, which changes the symmetry of the molecule from D_{4h} to D_{2h} . The overall symmetry of the resulting excited state is B_{2g} (in D_{2h}). The relaxation energy for this Jahn-Teller distortion is computed to be ~ 0.3 eV, and after relaxation the total energy is higher than the A_{1g} state by 20 meV. Despite this significant energy difference the distortion of the molecule is small: with the e_{gy} orbital singly occupied, in the Y direction the length increases by 0.004 Å and the Co-N bond elongates by 0.008 Å, while in the X direction the molecule is shortened by 0.01 Å and the Co-N bond length is reduced by 0.007 Å. Although these distortions are small one would expect them to have consequences for the vibrational modes of the molecule and to be resolvable in x-ray diffraction (XRD) or electron diffraction. The Raman spectra and gas-phase electron diffraction of MPCs are generally interpreted in terms of D_{4h} symmetry indicating an undistorted Co environment both in gas phase and in solution. The XRD patterns of CoPc films³⁷ also indicate that the four Co-N bonds are all equal to 1.910 Å. This evidence provides strong support for the idea of a robust A_{1g} ground state, stable in gas phase, solution, and thin film environments, in which the local Co geometry is undistorted and the degenerate e_g state is unoccupied. Attempts to converge a state with the b_{2g} orbital singly occupied were unsuccessful with the unconstrained SCF procedure converging to the state with the e_g orbital singly occupied; this behavior was also observed for calculations using the larger 6-31 + G* basis set.

Our finding that the E_g and A_{1g} states are close in energy (20 meV) and that there is a strong relaxation energy for the Jahn-Teller distortion of the E_g state (0.3 eV) are distinct from those of uncorrected GGA calculations which find the E_g state lower than the A_{1g} by 0.1 eV¹⁷ and ligand-field calculations which find the first orbital excited state to consist of a singly occupied b_{2g} orbital split from an A_{1g} ground state by ~ 43 meV.¹⁸

In order to compare the exchange interactions that would be expected from singly occupied e_g and a_{1g} orbitals, we have also computed the exchange interactions in both states in a molecular dimer with a geometry based on a stacking angle of 60° and a sliding angle of 0° (i.e., the thin-film geometry of Ref. 3). The exchange interaction for the state with the e_g orbital singly occupied is $J/k_B \sim 5$ K, which is much smaller than that computed for the state with a_{1g} orbital singly occupied $J/k_B \sim 60$ K. With a singly occupied a_{1g} orbital this calculated value in the dimer is close to the experimental spin-flip energy in the thin film,³ while with a singly occupied e_g orbital the calculation is an order of magnitude smaller. The observed strength of the magnetic coupling therefore also provides indirect evidence for the A_{1g} ground state.

B. CoPc one-dimensional chains

1. Band structure

In Figs. 5 and 6 the band structure, density of states (DOS), and spin densities are shown for CoPc chains in the α - and β -phase geometries, respectively. The wave vector component k is taken along the stacking axis and the zero of energy is chosen to be at midgap. In total 45 bands near the Fermi

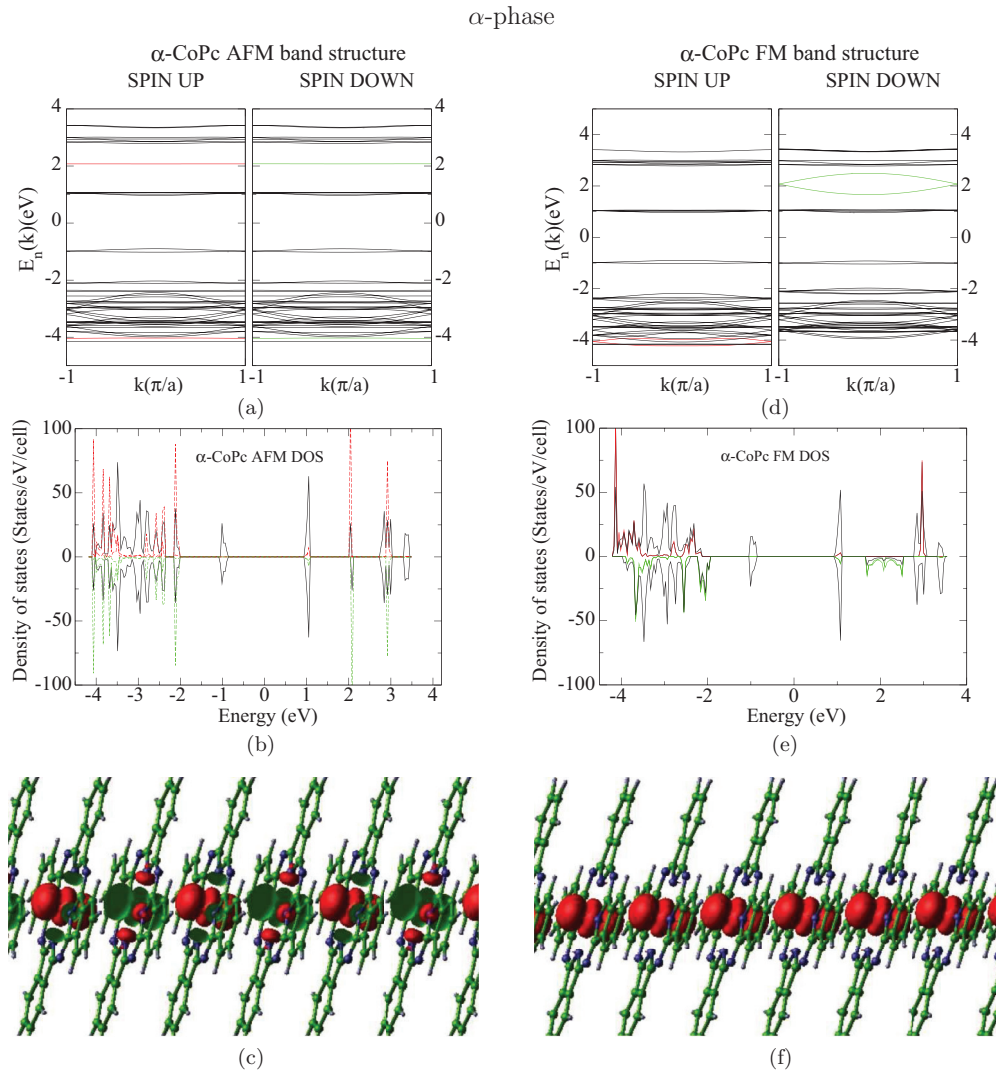


FIG. 5. (Color online) The band structure, density of states, and spin densities of AFM (left column) and FM (right column) configurations for α -phase CoPc are shown. In the band structure the a_{1g} -derived d bands in spin-up are highlighted in red, and the spin-down in green. In the density of states the spin-up is displayed as positive and spin-down as negative; the projected density of states (defined by a Mulliken procedure) for two Co atoms in the supercell is shown (red for spin-up, green for spin-down) scaled by a factor of 5.0 for clarity. The spin densities are constant-density contours where spin-up is in red and spin-down is in green. The isosurface value for the contour is set to $0.001e/\text{\AA}^3$.

energy are plotted; in the AFM configuration 34 states of each spin are occupied, while in the FM configuration there are 33 minority-spin and 35 majority-spin occupied bands. Band structures are plotted for the magnetic unit cell with lattice constant $\sim 7.5 \text{ \AA}$ ($\sim 9.6 \text{ \AA}$) for the α (β)-CoPc phases which is double that of the chemical unit cell.

The singly occupied d bands are identified by analyzing the Bloch orbitals in terms of atomic orbital contributions and also by comparing the band structure with the single-molecule electronic structure. As expected from the single-molecule calculations, the DFT single-particle band gap is dominated by the π orbitals of the Pc ligand and is $\sim 2 \text{ eV}$ for both α and β phases. The bands derived from the Co d states are almost flat in the AFM configuration (where the broken-symmetry condition localizes the spin-up and spin-down orbitals on different molecules and suppresses spin-conserving hybridization between the two) and have greater dispersion

in the FM configuration (where orbitals of the same spin are found on neighboring molecules and hybridization is possible), especially in the α phase. As in the single molecule the SOMO band is derived from the molecular a_{1g} orbital; these spin-up (spin-down) bands are shown in red (green) for clarity. The energy difference between the centroids of the occupied and empty a_{1g} derived bands gives an approximate measure of the effective Hubbard U , this time in the chain geometry; it is found to be approximately 6 eV for both α and β phases, in agreement with the value for the isolated molecule. The projected DOS on the two Co atoms is highlighted in red (green) for spin-up (spin-down). From the spin densities we can also tell that the singly occupied orbitals have a_{1g} symmetry.

The electronic structures of CoPc with other geometries share many similarities with α - and β -CoPc including band gap, effective Hubbard U , Mulliken charge densities on Co atoms, and Mulliken spin densities on Co atoms. However,

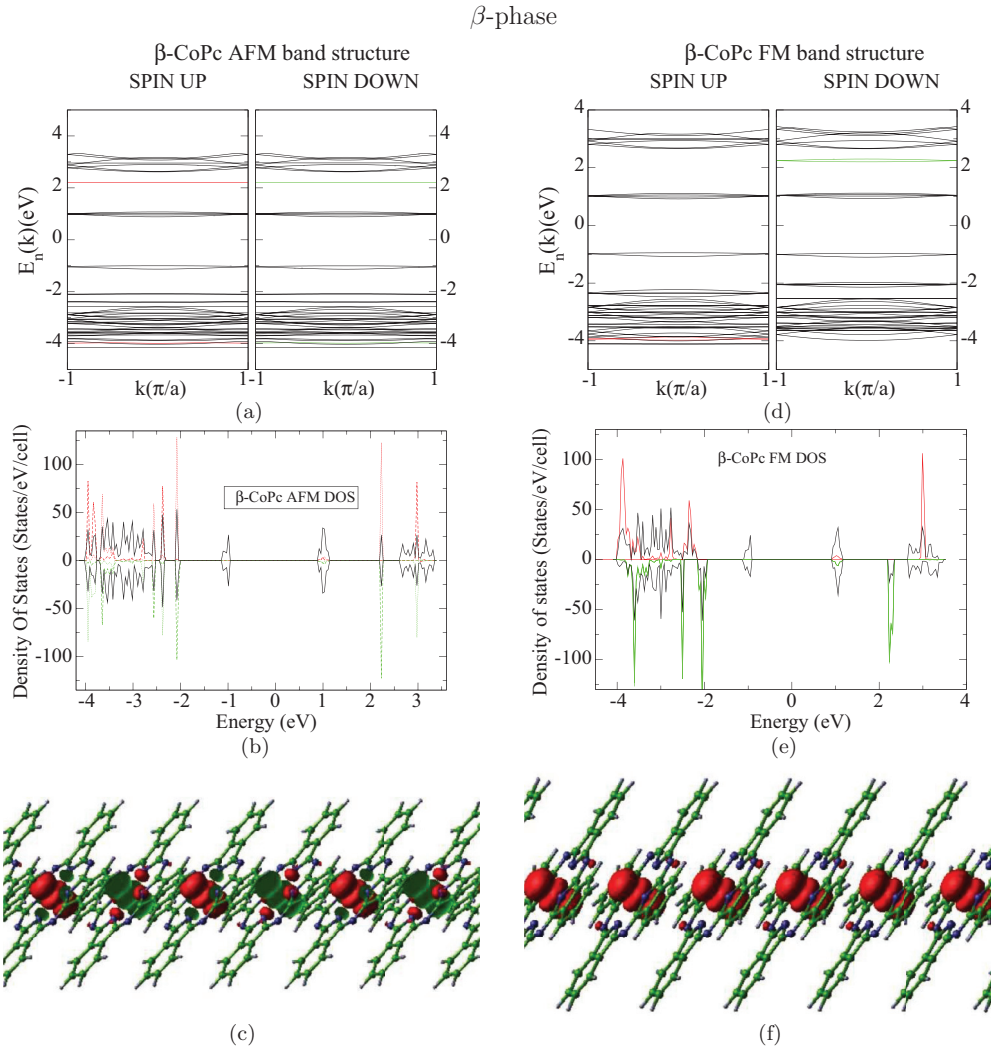


FIG. 6. (Color online) The band structure, density of states, and spin densities of AFM (left column) and FM (right column) configurations for β -phase CoPc are shown. In the band structure the a_{1g} -derived d bands in spin-up are highlighted in red, and the spin-down in green. In the density of states the spin-up is displayed as positive and spin-down as negative; the projected density of states (defined by a Mulliken procedure) for two Co atoms in the supercell is shown (red for spin-up, green for spin-down) scaled by a factor of 5.0 for clarity. The spin densities are constant-density contours where spin-up is in red and spin-down is in green. The isosurface value for the contour is set to $0.001e/\text{\AA}^3$.

the bandwidth closely related to the electron hopping between molecules varies as a function of geometrical parameter. For example, in α -CoPc FM configuration the bandwidth of the band derived from the a_{1g} orbital is ~ 0.5 eV and in β -CoPc is ~ 0.1 eV. For all the geometries calculated here, the variation of spin densities and the d_{z^2} orbital population on Co atoms is $< 2\%$. This provides strong evidence for the stability of the A_{1g} ground state as the intermolecular interactions are varied. As the E_g state is computed to be close in energy in the single molecule it is useful to estimate the variation in the relative stability of the states from the variation in the eigenvalues of the a_{1g} and e_g orbitals with stacking geometry. In the single molecule a_{1g} is ~ 1.3 eV lower in energy. In the molecular chain the splitting, estimated from the centroids of the related bands, is increased to ~ 1.4 eV for face-on stacking and to ~ 1.8 eV for the α , β , and η phases. This suggests that the stability of the A_{1g} ground state is enhanced by intermolecular interactions in the chain geometry.

2. Exchange interactions

The computed exchange interaction for α -phase CoPc is $J/k_B = 85$ K ($J/k_B = 1.75$ K in α -CuPc), and for the β phase $J/k_B = 2$ K ($J/k_B = 0$ in β -CuPc). These theoretical results are in quantitative agreement with recent magnetic measurements using superconducting quantum interference devices (SQUID)¹³ which find exchange couplings for α -CoPc of $J/k_B \sim 80$ K and for β -CoPc $J/k_B \sim 2$ K. For the thin-film geometry inferred from STM images³ we find $J/k_B = 61$ K (compare 105 ± 10 K measured by spin-flip spectroscopy, although there is some uncertainty in the stacking angle), and for the η phase of CoPc we predict $J/k_B \sim 80$ K. In Fig. 7 a logarithmic plot of the exchange interactions of CoPc for the full range of chain structures is shown as a function of the Co-Co distance (equivalent to the stacking angle) and the sliding angle. The dominant dependence of the exchange is on the stacking angle, with a peak of $J/k_B \sim 400$ K at a Co-Co distance of 3.42 Å (equivalent to $\phi = 90^\circ$), where

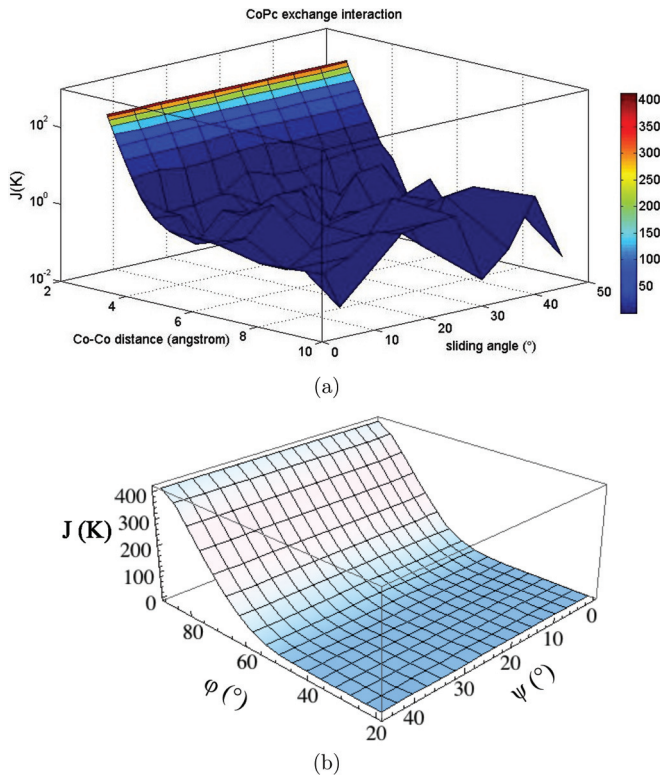


FIG. 7. (Color online) The structural dependence of exchange interactions is shown. In (a) $|J|$ is a function of Co-Co distance and the sliding angle is shown in a logarithmic plot. In (b) J is plotted as a function of stacking angle and sliding angle. Notice that (i) the peak value is approximately 400 K when the Co-Co distance = 3.42 Å equivalent to the stacking angle of 90° and (ii) from (b) the exchange interactions depend strongly on stacking angle, but weakly on sliding angle.

the molecules are directly face-on. This coupling is much larger than the maximum computed value of ~ 4 K in CuPc⁵ using very similar theoretical and numerical approximations. This raises the interesting possibility of room-temperature intrachain magnetic order if structures can be found with this packing. The magnetic coupling has a much weaker dependence on sliding angle which is illustrated by the similar interaction computed for the α and η phases.

The combination of strong dependence on stacking angle and weak dependence on sliding angle is similar to that found in calculations on CuPc.⁵ In CuPc it has been argued^{4,5} that the dominant interaction mechanism is indirect exchange¹² involving virtual spin polarization of the Pc ligand; this is because the superexchange pathways between Cu^{2+} are all strongly suppressed. Direct hopping of electrons between the single-occupied b_{1g} orbitals is small because these states lie in the molecular plane, while hopping via the ligand states is suppressed because those near the Fermi energy all have e_g or a_{1u} symmetry. In the case of CoPc, although hybridization of the d states with the ligands is still strongly suppressed by symmetry, the fact that the a_{1g} orbitals point along the normal to the molecular plane [see Figs. 5(c), 5(f), 6(c), and 6(f)] allows direct electron hopping between them, especially when the stacking angle is large, as manifested in the band picture by the significant dispersion of the empty (spin-down) a_{1g} states

in the α -phase structure [Fig. 5(d)]. In addition, as illustrated in Fig. 7, when the Co-Co distance is < 5 Å (equivalent to $\phi > 40^\circ$) the logarithmic plot of $|J|$ is a straight line, independent of sliding angle, corresponding to an exponential decay of the exchange with distance. This dependence strongly supports the suggestion that a direct-hopping superexchange mechanism is operating in CoPc for geometries in which significant overlap of the a_{1g} orbitals can occur. When the stacking angle is smaller than 40° , the exchange interactions start to fluctuate as a function of stacking and sliding angle, indicating the greater involvement of the ligand orbitals and suggesting a competition between superexchange and indirect exchange. We therefore speculate that the exchange interaction is dominated by direct superexchange when the stacking angle is large, with contributions from indirect exchange at small stacking angles. The averaged value of exchange interactions at small stacking angle is larger than those computed in CuPc, and the fluctuations occur with differently in the two materials⁵; this indicates that the superexchange might be dominant at small stacking angle as well.

We have analyzed the exchange mechanism by estimating the superexchange interaction (which is believed to be the dominant mechanism in CoPc) as $\frac{2t^2}{U}$, where $t = \frac{W}{4}$ with W being the width of singly occupied a_{1g} band and the Hubbard- U derived from the band structure as the splitting of the occupied and unoccupied a_{1g} derived d bands. This analysis of exchange interactions suggests that the superexchange contribution is dominant when the stacking angle is larger than 40° (Fig. 8), which is consistent with those results derived from the logarithmic plot in Fig. 7(a). The negative contribution from other exchange mechanisms might be dominated by either the direct exchange, owing to the large overlap between a_{1g} orbitals, or the indirect exchange. A more complete picture of the competition between the two mechanisms requires either model calculations⁴ or calculations that go beyond the single particle DFT approach and thus provide an analysis of

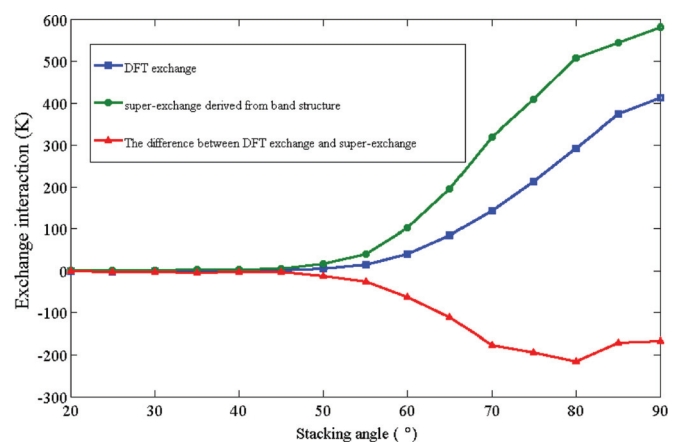


FIG. 8. (Color online) Exchange interactions arising from different mechanism is shown as a function of the stacking angle for the cross phase (the sliding angle is 45°). The exchange interactions computed using DFT is in blue, those arising from superexchange mechanism derived from the band structure are in green, and the exchange arising from other mechanisms including direct exchange and indirect exchange are in red. Notice that the superexchange is dominant in most of the stacking angles under investigation.

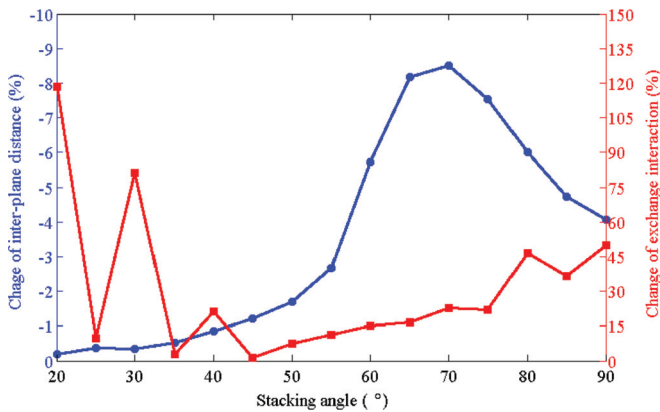


FIG. 9. (Color online) The changes of interplane distance and exchange interaction after optimizing the lattice constant as a function of the stacking angle at cross phase (the sliding angle is 45°) are shown. The interplane distance is reduced after geometrical optimization, and correspondingly the exchange increases. The largest change is at the stacking angle 70° .

interactions in terms of contributions to the many body wave function.⁴¹

Assuming that the effect of intermolecule interactions on intramolecular coordinates is negligible, we have optimized the lattice constant by combining the B3LYP functional with a long-range dispersion correction for the cross phases (for which the sliding angle is equal to 45°). As shown in Fig. 9, the optimization of the energy including the intermolecular Coulomb interaction and the van der Waals forces reduces the Co-Co distance (hence the interplane distance) relative to the experimental value by up to $\sim 8\%$ when the stacking angle is equal to 70° , and increases the exchange interaction by up to $\sim 120\%$ at a stacking angle of 20° . The exchange interactions are particularly sensitive to the interplane distance due to the out of plane orientation of the singly occupied d orbital. For the observed α -CoPc phase the calculated exchange interaction is increased by $\sim 8\%$ (~ 7 K).

We note that the Grimme dispersion correction appears to overestimate the van der Waals interaction since it produces interplanar distances shorter than those observed. The corresponding enhancements of the exchange may therefore also be overestimates.

V. CONCLUSION

Detailed calculations based on hybrid exchange density functional theory have confirmed the large intermolecular exchange interaction inferred for CoPc from electron tunneling

measurements.³ The calculations also suggest that the nearest-neighbor interaction could be significantly increased if the molecules could be brought to a fully face-on geometry. These exchange energies are unprecedentedly large for a TMPc with the spin localized on the transition metal, and suggest the possibility that intrachain magnetic correlations could be made strong at temperatures up to room temperature. This is particularly interesting when combined with the recent experimental observation that CoPc films behave as $S = \frac{1}{2}$ quantum spin chains,¹³ whose exchange interactions agree quantitatively with the values calculated here.

Our results also suggest that superexchange mediated by direct hopping between Co atoms in neighboring molecules is dominant when the stacking is larger than 40° , and indicate that there could be competition between superexchange of this kind and indirect exchange when the stacking angle is smaller than 40° . An estimate of the superexchange interaction suggests that it is the dominant contribution to the exchange mechanism. A more complete analysis of the contributions is not accessible at the DFT level and would require a calculation of the many body wave function. The estimated effective Hubbard U is large (about 6 eV). An empirical dispersion correction has been used to estimate the effects of van der Waals forces on the lattice constant and thus the exchange interactions. This suggests that the reduction of Co-Co distance due to the van der Waals forces significantly enhances the exchange interaction.

One of the by-products of this paper is the interesting electronic structure of isolated CoPc, and how it relates to the chains. Our calculations find that the A_{1g} state of the molecule has the lowest energy, and that it is stabilized relative to the competing states by the intermolecular interactions. Furthermore, the competing E_g state would imply a Jahn-Teller distortion and a much smaller exchange interaction, neither of which is observed.

For a large part of parameter space our theoretical predictions for the exchange interactions of CoPc still need to be tested by experiments. We hope this work will inspire experimentalists to search for new structures where the magnetic interactions may be even stronger, and to explore further the properties of organic-based quantum spin chains.

ACKNOWLEDGMENTS

We wish to acknowledge the support of the UK Research Councils Basic Technology Programme under Grant No. EP/F041349/1. We thank Gabriel Aeppli, Sandrine Heutz, Chris Kay, Michele Serri, Hai Wang, Marc Warner, and Zhenlin Wu for helpful discussions.

*w.wu@imperial.ac.uk

¹S. Heutz, C. Mitra, W. Wu, A. J. Fisher, A. Kerridge, A. M. Stoneham, A. H. Harker, J. Gardener, H.-H. Tseng, T. S. Jones, C. Renner, and G. Aeppli, *Adv. Mater.* **19**, 3618 (2007).

²H. Wang, S. Mauthoor, S. Din, J. A. Gardener, R. Chang, M. Warner, G. Aeppli, D. W. McComb, M. P. Ryan, W. Wu, A. J. Fisher, M. Stoneham, and S. Heutz, *ACS Nano* **4**, 3921 (2010).

³X. Chen, Y.-S. Fu, S.-H. Ji, T. Zhang, P. Cheng, X.-C. Ma, X.-L. Zou, W.-H. Duan, J.-F. Jia, and Q.-K. Xue, *Phys. Rev. Lett.* **101**, 197208 (2008).

⁴W. Wu, A. Kerridge, A. H. Harker, and A. J. Fisher, *Phys. Rev. B* **77**, 184403 (2008).

⁵W. Wu, A. J. Fisher, and N. M. Harrison, *Phys. Rev. B* **84**, 024427 (2011).

- ⁶Z. Bao, A. J. Lovinger, and J. Brown, *J. Am. Chem. Soc.* **120**, 207 (1998).
- ⁷S. Pramanik, C.-G. Stefanita, S. Patibandla, S. Bandyopadhyay, K. Garre, N. Harth, and M. Cahay, *Nat. Nano.* **2**, 216 (2007).
- ⁸M. Warner *et al.*, *Nature* (London) (submitted).
- ⁹G. A. Timco, S. Carretta, F. Troiani, F. Tuna, R. J. Pritchard, C. A. Muryn, E. J. L. McInnes, A. Ghirri, A. Candini, P. Santini, G. Amoretti, M. Affronte, and R. E. P. Winpenny, *Nat. Nano.* **4**, 173 (2009).
- ¹⁰J. S. Miller, A. J. Epstein, and W. M. Reiff, *Science* **240**, 40 (1988).
- ¹¹Z. H. Xiong, D. Wu, Z. Vally Vardeny, and J. Shi, *Nature* (London) **427**, 821 (2004).
- ¹²P. W. Anderson, *Phys. Rev.* **115**, 2 (1959).
- ¹³M. Serri *et al.*, *Nat. Mater.* (submitted).
- ¹⁴A. Zhao, Q. Li, L. Chen, H. Xiang, W. Wang, S. Pan, B. Wang, X. Xiao, J. Yang, J. G. Hou, and Q. Zhu, *Science* **309**, 1542 (2005).
- ¹⁵A. Zhao, Z. Hu, B. Wang, X. Xiao, J. Yang, and J. G. Hou, *J. Chem. Phys.* **128**, 234705 (2008).
- ¹⁶P. A. Reynolds and B. N. Figgis, *Inorg. Chem.* **30**, 2294 (1991).
- ¹⁷M.-S. Liao and S. Scheiner, *J. Chem. Phys.* **114**, 9780 (2001).
- ¹⁸T. Kroll, V. Yu. Aristov, O. V. Molodtsova, Yu. A. Ossipyan, D. V. Vyalikh, B. Büchner, and M. Knupfer, *J. Phys. Chem. A* **113**, 8917 (2009).
- ¹⁹S. Bhattacharjee, B. Brena, R. Banerjee, H. Wende, O. Eriksson, and B. Sanyal, *Chem. Phys.* **377**, 96 (2010).
- ²⁰B. Bialek, I. G. Kim, and J. I. Lee, *Thin Solid Films* **513**, 110 (2006).
- ²¹R. Ditchfield, W. J. Hehre, and J. A. Pople, *J. Chem. Phys.* **54**, 724 (1971).
- ²²M. J. Frisch *et al.*, GAUSSIAN 03 (Gaussian, Inc., Pittsburgh, PA, 1998).
- ²³M. Petersilka, U. J. Gossmann, and E. K. U. Gross, *Phys. Rev. Lett.* **76**, 1212 (1996).
- ²⁴R. E. Stratmann and G. E. Scuseria, *J. Chem. Phys.* **109**, 8218 (1998).
- ²⁵R. Dovesi, V. R. Saunders, C. Roetti, R. Orlando, C. M. Zicovich-Wilson, F. Pascale, B. Civalleri, K. Doll, N. M. Harrison, I. J. Bush, P. D'Arco, and M. Llunell, CRYSTAL09 User's Manual (University of Torino, Torino, 2009).
- ²⁶H. J. Monkhorst and J. D. Pack, *Phys. Rev. B* **13**, 5188 (1976).
- ²⁷A. D. Becke, *J. Chem. Phys.* **98**, 5648 (1993).
- ²⁸F. Illas, I de P. R. Moreira, C. de Graaf, and V. Barone, *Theor. Chem. Acc.* **104**, 265 (2000).
- ²⁹J. Muscata, A. Wanderb, and N. M. Harrison, *Chem. Phys. Lett.* **342**, 397 (2001).
- ³⁰L. Ge, B. Montanari, J. H. Jefferson, D. G. Pettifor, N. M. Harrison, and G. A. Briggs, *Phys. Rev. B* **77**, 235416 (2008).
- ³¹J. K. Perry, J. Tahir-Kheli, and W. A. Goddard, *Phys. Rev. B* **63**, 144510 (2001).
- ³²I. P. R. Moreira, F. Illas, and R. L. Martin, *Phys. Rev. B* **65**, 155102 (2002).
- ³³S. Grimme, *J. Comput. Chem.* **27**, 1787 (2006).
- ³⁴L. Noodleman, *J. Chem. Phys.* **74**, 5737 (1981).
- ³⁵W. Heisenberg, *Z. Phys.* **49**, 619 (1928).
- ³⁶J. M. Assour and W. K. Kahn, *J. Am. Chem. Soc.* **87**, 207 (1965).
- ³⁷P. Ballirano, R. Caminiti, C. Ercolani, A. Maras, and M. A. Orrú, *J. Am. Chem. Soc.* **120**, 12798 (1998).
- ³⁸M. Brinkmann, P. Turek and J.-J. André, *J. Mater. Chem.* **8**, 675 (1998).
- ³⁹A. K. Gregson, R. L. Martin, and S. Mitra, *J. Chem. Soc. Dalton Trans.* **1976**, 1458 (1976).
- ⁴⁰R. Seoudi, G. S. El-Bahy, and Z. A. El Sayed, *Opt. Mat.* **29**, 304 (2006).
- ⁴¹J. Cabrero, N. Ben Amor, C. de Graaf, F. Illas, and R. Caballol, *J. Phys. Chem. A* **104**, 9983 (2000).